JOURNAL OF MATERIALS SCIENCE 19 (1984) 4007–4013

The influence of quenched-in crystals on the thermal stability of partially amorphous $Zr_{76}Ni_{24}$ alloy*

B. TOLOUI
Oxford Research Unit, The Open University, Foxcombe Hall, Boars Hill, Oxford, OX1 5HR, UK

G. GREGAN
Department of Metallurgy, University of Sheffield, Mappin Street, Sheffield, S1 3JD, UK

M. G. SCOTT
Standard Telecommunication Laboratories Ltd, London Road, Harlow, Essex, CM17 9NA, UK

Fully glassy and part-crystalline ribbons were prepared by melt spinning the $Zr_{76}Ni_{24}$ melt at different rates. X-ray and STEM studies confirmed that the quenched-in crystals are α-zirconium. It is shown that these pre-existing crystals do not grow during annealing treatment nor do they act as heterogeneous nucleation sites, and remain inertly during the crystallization of the surrounding amorphous matrix. Crystallization studies showed that the existence of a fraction of crystallinity within the glassy matrix increases the stability of the matrix against further crystallization. Possible explanations for this behaviour are presented.

1. Introduction

The science and technology of metallic glasses is now well established and the scientific literature abounds with reports on the structure, properties and stabilities of these materials [1, 2]. Unlike familiar glass systems, metallic glasses suffer from relative instability against crystallization. Crystal nucleation and growth rates are high in metal alloys and as a consequence it is impossible to heat metal glasses much above $0.5T_m$ (where T_m is the melting point) without inducing spontaneous crystallization [3]. For the same reason many useful metallic glasses have a limited stability, even at temperatures as low as 383 K [4]. Such proneness to crystallization places severe limits on the operating environments of what promises otherwise to be a useful class of materials. However, from a scientific angle, metallic glasses do provide a unique opportunity to study crystal nucleation and growth in an isotropic medium. Many investigations [5, 6] have indicated that the crystallization reactions in metallic glasses are similar to those in undercooled liquids just below the melting point and that the kinetics are characterized by the standard equations for solid state phase transformation. It has been established that the crystallizing phases are often non-equilibrium and grow with a highly faulted morphology. There is some debate about the nature of the nucleation process, particularly about the competing roles of transient nucleation within the glass and the athermal growth of quenched-in nuclei [7]. To date little attention has been paid to the role of heterogeneous nucleation sites. It has been reported [5] that crystallization may be initiated at ribbon surfaces, though this may be a consequence of compositional inhomogeneities rather than genuine nucleation. It is clear that the

*Work carried out while the authors were in the University of Sussex, School of Engineering and Applied Sciences, Brighton, BN1 9QT, UK.

0022–2461/84 $03.00 + .12

alternative potential nucleation sites are quenched-in crystals within the amorphous matrix. Since part-crystalline materials have assumed an importance on account of their promise as high-frequency low loss magnetic materials [8] it is important to understand the influence of the crystals on thermal stability of the microstructure. It is the objective of this paper to report and discuss the results, which were partly presented in a previous paper [9] of the effects of quenched-in (pre-existing) crystals on the thermal stability of partially amorphous $Zr_{76}Ni_{24}$ alloy. The choice of a Zr–Ni alloy was not for any technological reason but simply because we have a wide experience of these alloys [10, 11] and their crystallization behaviour is relatively simple [11].

2. Experimental procedure

The zirconium-24 at% nickel alloy was made by induction heating high purity zirconium and nickel in a water-cooled silver boat under a pure argon flow. The ingots were broken and remelted several times in order to ensure compositional homogeneity, which was confirmed by microprobe analysis. Glassy ribbons ~4 mm wide and approximately 50 μm thick were produced by melt-spinning technique at different wheel rotation rates and ejection pressures so as to form either fully amorphous or part-crystalline ribbons. To achieve this, approximately 4 g charges of the alloy were melted in a quartz crucible and ejected through a 1 mm diameter orifice onto the external surface of a rotating 150 mm diameter copper wheel. Completely amorphous and partially crystalline ribbons were produced at a wheel rotation of 4500 rpm with ejection pressure 80 Pa, and 3000 rpm, with ejection pressure 55 Pa, respectively. After sealing in argon-filled quartz ampoules, specimens were annealed in a non-inductively wound tube furnace. The structures of the two types of ribbon were examined by X-ray diffraction using Co$K\alpha$ radiation. Prior to X-ray diffraction the ribbons were lightly abraded and swabbed with a mixture of nitric acid (2.5 ml), hydrofluric acid (5 ml) and glycerol (92.5 ml) to remove any surface contamination. For transmission electron microscopy the specimens were thinned by the window technique using a 35:65:200 parts by volume mixture of perchloric acid, *n*-butanol and methanol at -60°C. The specimens were examined by a JEOL 120C fitted with a JEOL TEMSCAN and LINK system for chemical analysis. Calorimetry was carried out in the differential scanning calorimetry (DSC) cell of a Dupont 1090 Thermal Analyser at heating rates between 5 and 80 K min^{-1} and isothermal heating between 580 and 630 K was employed. Typically 5 to 10 mg of sample were used for dynamic experiments and 20 to 25 mg for isothermals. In each case the samples were packed tightly in sealed aluminium cans and an empty can was used as the reference. The temperature and heat flow axes were calibrated using the melting endotherm of zinc.

3. Results

3.1. X-ray diffraction

X-ray diffraction was performed on the two types of ribbon after their production. The amorphous ribbon showed a broad maximum centred at $2\theta = 42^\circ$ with no sharp peaks characteristic of any crystalline fraction. By contrast the more slowly cooled ribbons showed a set of well-defined crystalline peaks superimposed on an amorphous pattern in which the maximum was slightly shifted with respect to that in amorphous specimens. The crystalline peaks could be fitted to a hexagonal close-packed structure with lattice parameters $a = 0.326$, $c = 0.522$ nm (both ± 0.002 nm). These values are slightly larger than those of pure α-zirconium ($a = 0.323$, $c = 0.515$ nm) and on this evidence we assumed that the crystals were α-zirconium with some nickel in solid solution. Since the equilibrium solubility of nickel in α-zirconium is negligible and no data for metastable solid solution exist it was not possible to deduce the composition of the α-Zr(Ni) crystals from lattice parameters.

Representative samples of the two types of ribbon were heat-treated in a tube furnace and examined by X-ray diffraction technique. X-ray diffractograms from initially amorphous samples indicated that the crystallizing phase was C16 tetragonal type, though the line positions were shifted with respect to those of stoichiometric Zr_2Ni, suggesting that the phase can form off-stoichiometrically. Only after long anneals did any reflections from the other equilibrium phase, α-zirconium, appear. Ribbons which initially contained α-zirconium crystals behaved in a similar fashion though the diffraction patterns were inevitably more complex.

3.2. Electron microscopy

The amorphous ribbons were featureless save for

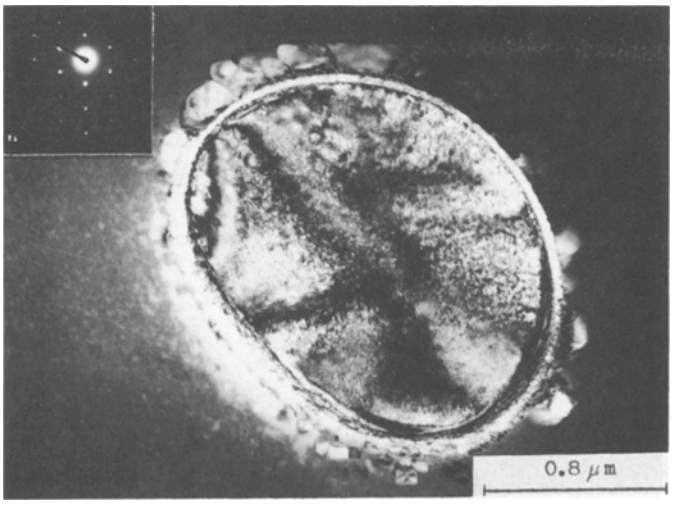

Figure 1 Transmission electron micrograph of part-crystalline ribbon.

the mottled appearance which appears to be a polishing artefact in this type of material. The part-crystalline ribbon exhibited an amorphous matrix with a random distribution of non-faceted crystals. Fig. 1 shows a typical transmission electron micrograph and diffraction pattern of part-crystalline ribbons Scanning electron microscope (SEM) micrographs confirmed that these crystals were distributed uniformly through the ribbon thickness. Each consisted of a central core, typically a few micrometres in diameter, a thin surrounding rim and a collection of smaller crystals which appeared to have nucleated on the central core. Diffraction patterns from the core could always be indexed as h c p with a lattice parameter close to that of α-zirconium. Quantitative X-ray microanalysis confirmed that in all cases these areas were highly zirconium rich with respect to the surrounding amorphous matrix. No unambiguous diffraction or composition information could be obtained from the rim and other surrounding crystals; however, any "stray" spots in the diffraction patterns could be indexed as Zr_2Ni.

Electron microscopy was also carried out on the heat-treated samples of the two types of ribbon. In the fully amorphous specimens small irregular shaped crystals nucleated and grew at random within the matrix. The diffraction patterns from these crystals were consistent with a C16 structure. Energy-dispersive X-ray (EDX) analysis indicated that they had a composition close to that of the matrix. Similar crystals formed in the amorphous matrix of the initially part-crystalline samples. Fig. 2 shows a bright field TEM micrograph of the heat-treated sample (50 min at 593 K). A notable feature was the absence of any further heterogeneous nucleation on the quenched-in crystals; rather in many cases such as shown in Fig.

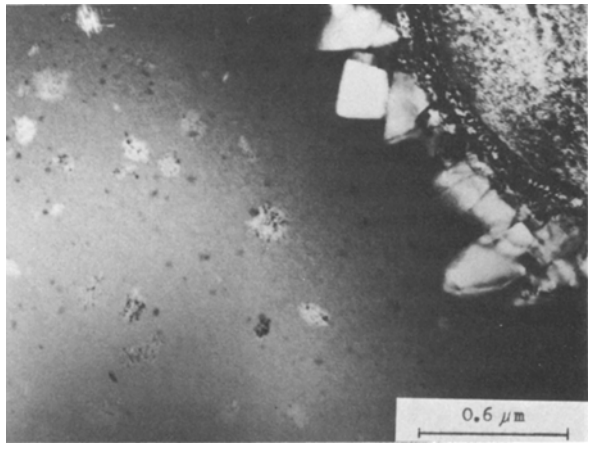

Figure 2 Transmission electron micrograph of initially part-crystalline sample annealed 50 min at 593 K.

TABLE I DSC continuous heating data

Rate (K min^{-1})	T_x (K)		ΔH (kJ mol^{-1})		% cryst.
	Amorphous	Part-crystalline	Amorphous	Part-crystalline	
5	628.3	642.2	5.34	4.91	11.8
10	636.7	648.9	5.46	4.85	11.2
20	646.2	655.1	5.65	4.97	12.0
40	655.5	664.0	5.86	5.16	11.9
80	666.2	673.3	6.02	5.33	11.5

2, there was a noticeable precipitation-free zone around the α-zirconium crystals, which we conclude act inertly during the crystallization of the surrounding amorphous matrix.

3.3. DSC

Fig. 3 shows typical DSC thermograms obtained from the two types of ribbon. In both cases and at all heating rates crystallization was accompanied by a single exotherm; however, in the partially crystalline samples the peak had a slight high temperature tail and occurred at higher temperatures than in the fully amorphous ones. From the area under the exotherms the respective heats of crystallization were determined and by simple ratio the fraction of crystallinity in the part-crystalline samples were calculated as 0.12 ± 0.01. Overall activation energies for the crystallization process were estaimated from Kissinger's expression [12] by plotting $\ln(T_p^2/\beta)$ against $1/T_p$, where T_p is the peak temperature of the crystallization exotherm at a heating rate, β. The value for the partially crystalline samples 305 ± 5 kJ mol^{-1}, was significantly larger than that for the fully amorphous samples, 255 ± 5 kJ mol^{-1}. Tables I and II summarize the data obtained from DSC experiments for continuous and isothermal heating, respectively. From the isothermal anneals' data again it is evident that the partially crystallized samples were more stable against crystallization than the fully amorphous ones, for example at 613 K an initially fully amorphous sample was fully crystallized after 8 min, whereas a sample which inintially contained some α-zirconium crystals was only just beginning to crystallize after the same time. The isothermal DSC thermograms were used to determine the kinetics of crystallization. The fraction transformed, $z(t)$, at a time, t, was taken as proportional to the partial area up to that time under the crystallization exotherm. These data were then fitted to the Johnson–Mehl–Avrami equation which is satisfied by many solid state nucleation and growth processes [13] including the crystallization of metallic glasses [6]:

$$z(t) = 1 - \exp[-k(t - t_0)^n] \quad (1)$$

where k is a rate constant, t_0 is an incubation time taken as the time for the onset of crystallization and n an exponent which may be obtained from the slope of a plot of $\ln\{-\ln[1 - z(t)]\}$ against $(t - t_0)$. Representative examples are shown in Fig. 4. In all cases $3 < n < 4$ with a tendency for the lowest values of n in part-crystalline specimens.

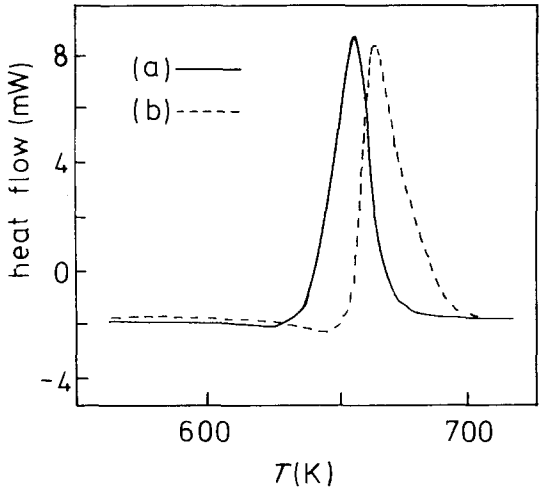

Figure 3 DSC thermograms of (a) amorphous, (b) part-crystalline samples. Heating rate 40 K min^{-1}.

TABLE II DSC isothermal heating data

Temp (K)	Amorphous		Part-crystalline	
	Time (min)		Time (min)	
	Start, t_s	Finish, t_f	Start, t_s	Finish, t_f
583	35.0	110.0	–	–
593	18.0	54.0	–	–
603	2.0	18.0	27.5	93.5
608	–	–	17.0	60.0
613	0.5	8.0	7.3	36.0
618	–	–	2.7	23.4
623	–	–	0.5	15.7

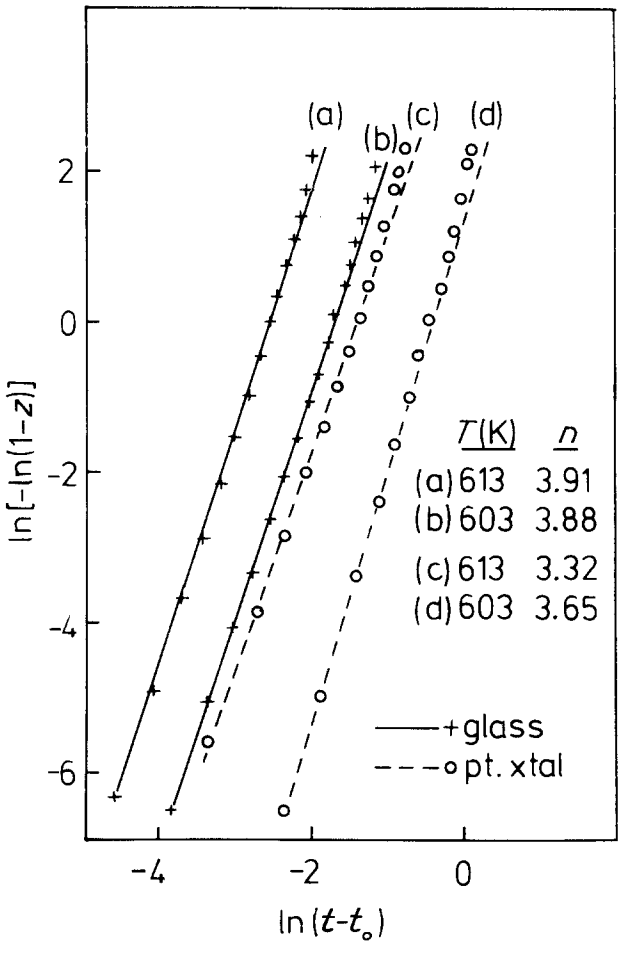

Figure 4 Fit of isothermal crystallization kinetics to Johnson–Mehl–Avrami equation at two temperatures. "n" is the Avrami exponent.

4. Discussion

Under equilibrium conditions the nickel–zirconium alloy in question solidifies eutectically to β-zirconium (b c c) and Zr_2Ni (C16); below 1113 K the β-zirconium transforms martensitically to the α (h c p) polymorph. The solubility of nickel in α-zirconium is negligible. It is clear that in the present work these equilibrium reactions are suppressed and that they control neither the kinetics of glass formation nor those of subsequent crystallization. More significantly there is a distinct difference between the crystals produced during rapid solidification (α), and which therefore must be avoided if a glass is to be formed, and those produced during subsequent annealing of the glass (Zr_2Ni). Accordingly correlation need not be expected between ease of glass formation and glass stability. Indeed, whilst it has been shown that there is a local minimum in the critical cooling rate against composition curve at 75 at % Zr [14], the crystallization temperature and activation energy both decrease monotonically with increasing zirconium content in glasses containing more than 50 at % Zr [10]. Three origins of the α-crystals can be proposed:

(a) β-zirconium crystals grown in the undercooled melt may have decomposed subsequently either martensitically or by the displacive ω-transformation. The fault free appearance of the α-crystals, however, is inconsistent with a martensitic transformation and, whilst ω-phase has been reported as the decomposition product of the amorphous $Zr_{75}Cu_{25}$ phase [15], the diffraction data given in [15] bore no resemblance to our diffraction patterns which could all be indexed as hexagonal close-packed. Nevertheless the bright field micrographs of some of the crystals did have a mottled appearance which may be indicative of some fine scale precipitation.

(b) It is well known that when the ribbon leaves the rotating substrate during the melt spinning process it is still at a temperature well above room

temperature [16]. During the subsequent, slower, air cooling it is quite feasible that some crystallization of an initially glassy material may occur. However, in view of the observations to date [10, 11] that the crystallization product of zirconium-rich Zr–Ni glasses is invariably the C16 Zr_2Ni phase, autotempering between T_g and room temperature does not seem a likely origin of the α-crystals.

(c) We are left then with the conclusion that the α-zirconium crystals nucleated and grew directly within the undercooled melt and that the remaining liquid vitrified when T_g was reached. Since the equilibrium phase is β, such direct nucleation of α would require an undercooling of at least 120 K; such undercoolings are readily achievable by rapid solidification.

The formation of a primary phase with rejection of solute as a precursor to glass formation is at variance with the prediction of Massalski [17] that, depending on the T_0 temperature, suppression of the eutectic can lead only to a glass or to diffusionless solidification of the terminal phase. Indeed, diffusionless solidification of a b c c Zr(Ni) solid solution in the same alloy has been reported elsewhere [18]. However, Massalski considers only crystal growth and takes no account of the relative nucleation rates of the competing phases. In view of the rejection of solute which has occurred it is surprising that the α-crystals did not adopt a dendritic morphology, particularly in the light of the observation that β-dendrites have been observed in the same glass [19]. Dendritic growth occurs when [20]:

$$\frac{mC_0}{D}\frac{(1-K_0)}{K_0} > \frac{G}{v} \qquad (2)$$

where m is the slope of the liquidus, C_0 is the overall alloy composition, K_0 the partition coefficient, D the diffusion coefficient, G the temperature gradient and v the growth rate. Taking values of m, C_0, K_0 from the Ni–Zr equilibrium diagram and assuming a liquid diffusion coefficient of about $10^{-9}\,m^2\,sec^{-1}$, the left hand side of the equation has a value between 10^{11} and $10^{12}\,K\,m^{-2}\,sec$. With a maximum temperature gradient, G, of the order of $10^7\,K\,m^{-1}$ dendritic growth is predicted at velocities up to 10^4 to $10^5\,m\,sec^{-1}$, much larger than those experienced during splat-quenching (10^{-2} to $10^{-1}\,m\,sec^{-1}$). We can offer, therefore, no satisfactory explanation for the lack of dendritic growth. Finally, no unambiguous identification could be made of the "rim" and other crystals surrounding the α-zirconium cores, although any "stray" spots in the electron diffraction patterns were indexable as Zr_2Ni. We can only speculate that they nucleated heterogeneously in the zirconium depleted region; it is not clear whether this occurred above or below T_g.

There is some disagreement about the phases produced during crystallization of fully amorphous $Zr_{76}Ni_{24}$ alloy. Buschow and Beckmanns [21] have claimed that a metastable β-Zr(Ni) solution is formed. The behaviour reported here is, however, at variance with this and consistent with our own earlier observations. The matrix decomposed by the random nucleation and growth of highly faulted crystals with C16 tetragonal structure. The decomposition mode was polymorphic with the C16 phase forming well away from the Zr_2Ni stoichiometry. The kinetics of crystallization was well fitted by the Johnson–Mehl–Avrami equation; the exponent of approximately 4 was consistent with a process in which both nucleation and growth rates were independent of time. Instinctively one might expect the presence of a sizeable percentage of quenched-in crystals to reduce the stability of the glass against further crystallization. This might arise for one of three reasons: the activation energy for growth of the existing crystals may be lower than that for nucleation and growth of new crystals within the glassy matrix; the existing crystals may act as heterogeneous nucleation sites for further crystallization; the lower quench rate required to produce the partially crystalline material may lead to a higher population of quenched-in nuclei and therefore facilitate subsequent crystallization. In practice none of the above occurs in the present case and the part-crystalline material is in fact more stable than the fully amorphous. A self-consistent explanation is as follows. Since the quenched-in crystals are rich in zirconium the surrounding matrix must be nickel rich with respect to the overall alloy composition. As has been shown elsewhere [10] both the crystallization temperature, T_x, and activation energy, E_x, increase monotonically with increasing nickel content. The matrix therefore has a higher T_x and in the absence of other effects will appear more stable than glasses of the nominal alloy composition. Indeed, from previous data [20] we can show that an increase of about 12 K in T_x at a heating rate of $10\,K\,min^{-1}$ is equivalent to an increase in nickel content from 24 to about

27 at %. If we assume that the matrix is homogeneous and that the crystals are close to pure zirconium a simple mass balance calculation gives a percentage crystallinity of about 12%, which is in excellent agreement with the value determined calorimetrically. In practice of course the matrix is unlikely to be compositionally homogeneous and the highest nickel content is expected in the immediate vicinity of the α-zirconium crystals. Using the same arguments as above this region should be the most resistant to crystallization, so giving rise to the observed precipitate-free zone in Fig. 2. Aside from this precipitate-free region the matrix behaves independently of the quenched-in crystals and morphologically the crystallization process is identical to that described above for fully amorphous specimens. In view of the fact that the matrix is unlikely to be homogeneous the fit of the kinetics to the Johnson–Mehl–Avrami equation is surprisingly good. The lower value of the exponent is possibly indicative of a greater contribution of quenched-in nuclei and therefore nucleation-site exhaustion. Such a behaviour is consistent with the lower cooling rate needed to make these samples.

5. Conclusions

We have shown that in $Zr_{76}Ni_{24}$ at least the crystallization process that limits glass formability is not the same as that which determines the subsequent stability of the glass. The presence of the quenched-in α-crystals within the glassy matrix increases the stability of the matrix against further crystallization. This behaviour is believed to be a consequence of nickel rejection from the quenched-in crystals. There is no evidence for further growth of the pre-existing crystals during heat treatment nor do they act as heterogeneous nucleation sites.

Acknowledgements

We wish to thank both the Science and Engineering Research Council and the U.S. Office of Naval Research for support of this programme of research on metallic glasses.

References

1. "Glassy Metals I", edited by H. J. Guntherodt and H. Beck (Springer Verlag, Heidelberg, 1981).
2. Proceedings of the 4th International Conference on Rapidly Quenched Metals, edited by T. Masumoto and K. Suzuki (Japan Institute of Metals, Sendai, 1982).
3. M. G. SCOTT, in "Rapidly Quenched Metals III", edited by B. Cantor (The Metals Society, London, 1978) p. 191.
4. F. E. LUBORSKY, in Proceedings of the 2nd International Symposium on Amorphous Magnetism, edited by R. Levy and R. Hasegawa (Plenum, New York, 1976).
5. U. KOSTER and U. HEROLD, in "Glassy Metals I", edited by H. J. Guntherodt and H. Beck (Springer Verlag, Heidelberg, 1981) p. 225.
6. M. G. SCOTT, in "Amorphous Metallic Alloys", edited by F. E. Luborsky (Butterworths, London, 1983).
7. U. KOSTER and U. HEROLD, in The Proceedings of the 4th International Conference on Rapidly Quenched Metals, edited by T. Masumoto and K. Suzuki (Japan Institute of Metals, Sendai, 1982) p. 717.
8. A. DATTA, N. J. DECRISTOFARO and L. A. DAVIS, *ibid.* p. 1007.
9. B. TOULOUI, G. GREGAN and M. G. SCOTT, *J. Non-Crystall. Solids* **61/62** (1984) 1009.
10. Y. D. DONG, G. GREGAN and M. G. SCOTT, *ibid.* **43** (1981) 403.
11. M. G. SCOTT, G. GREGAN and Y. D. DONG, in The Proceedings of the 4th International Conference on Rapidly Quenched Metals, edited by T. Masumoto and K. Suzuki (Japan Institute of Metals, Sendai, 1982) p. 271.
12. H. E. KISSINGER, *Anal. Chem.* **29** (1957) 1702.
13. J. BURKE, "The Kinetics of Phase Transformations in Metals" (McGraw-Hill, London, 1969) p. 170.
14. Y. NISHI, T. MOROHASHI, N. KAWAKAMI, K. SUZUKI and T. MASUMOTO, in The Proceedings of the 4th International Conference on Rapidly Quenched Metals, edited by T. Masumoto and K. Suzuki (Japan Institute of Metals, Sendai, 1982) p. 111.
15. R. V. RAMAN, PhD thesis, North Eastern University (1977).
16. H. A. DAVIES, in "Rapidly Quenched Metals III", edited by B. Cantor (The Metals Society, London, 1978) p. 1.
17. T. B. MASSALSKI, in The Proceedings of the 4th International Conference on Rapidly Quenched Metals, edited by T. Masumoto and K. Suzuki (Japan Institute of Metals, Sendai, 1982) p. 203.
18. R. RAY, PhD thesis, North Eastern University (1968).
19. S. BANERJEE, Unpublished work.
20. W. A. TILLER, K. A. JACKSON, J. W. RUTTER and B. CHALMERS, *Acta. Metall.* **1** (1953) 428.
21. K . H. BUSCHOW and N. BECKMANNS, *Phys. Rev. Lett.* **1319** (1979) 3843.

Received 5 January
and accepted 8 February 1984